Electric Supplementary Information (ESI) on
Mutual effect of Cs(I) and Sr(II) sorption on nano-talc investigated by EXAFS, modeling and theoretical calculations

Yubing Sun[a], Wencheng Song[a], Yang Liu[a], Tasawar Hayat[b], Ahmed Alsaedi[b], Yuejie Ai[a]*, Virender K. Sharma[c], Xiangke Wang[a, c]*

[a] *MOE Key Laboratory of Resources and Environmental System Optimization, College of Environmental Science and Engineering, North China Electric Power University, Beijing 102206, P.R. China*

[b] *NAAM Research Group, Department of Mathematics, Faculty of Science, King Abdulaziz University, Jeddah 21589, Saudi Arabia*

[c] *School of Public Health, Texas A&M University, Texas 77843, USA*

[d] *Collaborative Innovation Center of Radiation Medicine of Jiangsu Higher Education Institutions, School for Radiological and Interdisciplinary Sciences, Soochow University, Suzhou 215123, P.R. China*

sunyb@ipp.ac.cn (Y. Sun); wencsong@cmpt.ac.cn (W. Song); tahaksag@yahoo.com (T. Hayat); aiyuejie@ncepu.edu.cn (Y. Ai); vsharma@sph.tamhsc.edu (Virender K. Sharma); xkwang@ncepu.edu.cn(X. Wang).

Preparation of FT-IR, XPS and EXAFS samples

The samples for FT-IR and XPS analysis was prepared as followed procedures: 3.0 mL of 0.1 mol/L $NaClO_4$ solution and 15 mL of 20.0 mg/L Sr(II) or Cs(I) solutions (7.5 mL of 20.0 mg/L Sr(II) and 7.5 mL of 20.0 mg/L Cs(I) solutions for competitive adsorption) were added into 50 mL polycarbonate tubes, and then 12 mL of 5.0 g/L talc suspensions were provided. pH values of suspension were adjusted 5.0 by adding negligible volume of 0.1-5.0 mol/L $HClO_4$ or NaOH solution. Then suspension was agitated on a shaker for a reaction time of 48 h. The solid and liquid phases were separated by centrifugation at 7710 ×*g* for 30 min. The samples for IR and XPS analysis were obtained by drying them in vacuum oven overnight. The samples for EXAFS analysis of Sr(II)-bearing talc at pH 5.0 were prepared as the following protocols: the talc and $NaClO_4$ (0.01 mol/L ionic strength) were weighted into 250 mL flask bottles and then Milli-Q water was pre-equilibrated for 24 h. The $Sr(NO_3)_2$ or $CsNO_3$ solution (m/V = 2.0 g/L) were dropwise added under vigorous stirring conditions, and the solution were adjusted to pH 5.0 by using neglected volume 0.01-1.0 mol/L $HClO_4$ or NaOH solution. Samples were then gently agitated on a shaker for 2 days. The solid phase was separated from liquid phase by centrifuging it at 7710 × *g* for 30 min and then through 0.22-μm membrane filters. The wet pastes of Sr(II)-bearing talc were mounted in Teflon sample holders with Kapton tape.

Selected properties of talc

The constitutes (%), N_2-BET surface area, protonation and deprotonation constants (log K^+ and log K^-) of talc were showed in Table S1.

Table S1 The Selected Properties of Talc Samples

Talc constitutes (%)	S_{BET} (m^2/g)	Average pore diameter (nm)	Log K^+	Log K^-
SiO_2 (63.65), MgO (30.63) FeO(0.24), Al_2O_3 (0.54), CaO(0.32), K_2O (0.1), Na_2O (0.1)	10.23	6.67	4.69	-6.06

Table S2. The constitutes of simulant groundwater (#1) and seawater (#2)[S1]

Constitutes of #1	Concentration (mg/L)	Constitutes of #2	Concentration (mg/L)
Ca^{2+}	100	Na^+	8050
Mg^{2+}	6.3	Mg^{2+}	930
Na^+	25	Ca^{2+}	305
Sr^{2+}	0.8	K^+	295
Cs^+	0.5	Sr^{2+}	7.5
Cl^-	236	Cs^+	0.5
CO_3^{2-}	0.9	Cl^-	10410
SO_4^{2-}	0.9	CO_3^{2-}	210

Characterization

The morphology of magnesium silicate was illustrated by scanning electron microscopy (SEM, JSM-6700F field emission scanning electron microscope, JEOL). The mineralogy of magnesium silicate was identified by X-ray diffraction (XRD, D/Max-Ra X-ray diffraction spectrometer, RIGAKU) with graphite monochromatized Cu-$K\alpha$ radiation at 2 °/min of scan speed and 0.02° of step size. The surface functional groups of magnesium silicate were confirmed using Fourier transform infrared spectrometer (FT-IR, JASCO FT-IR 410 spectrophotometer). Samples for FTIR analysis were prepared by adding 2.0 mg of magnesium silicate into 0.098 g KBr disks. The total elemental analyses of magnesium silicate were performed with an inductively coupled plasma- optical emission spectrometer (ICP-OES, Nippon Jarrell-Ash). The values of ζ-potential (mV) were determined at least three measurements for each pH (pH 2-11, I = 0.01 mol/L $NaClO_4$).

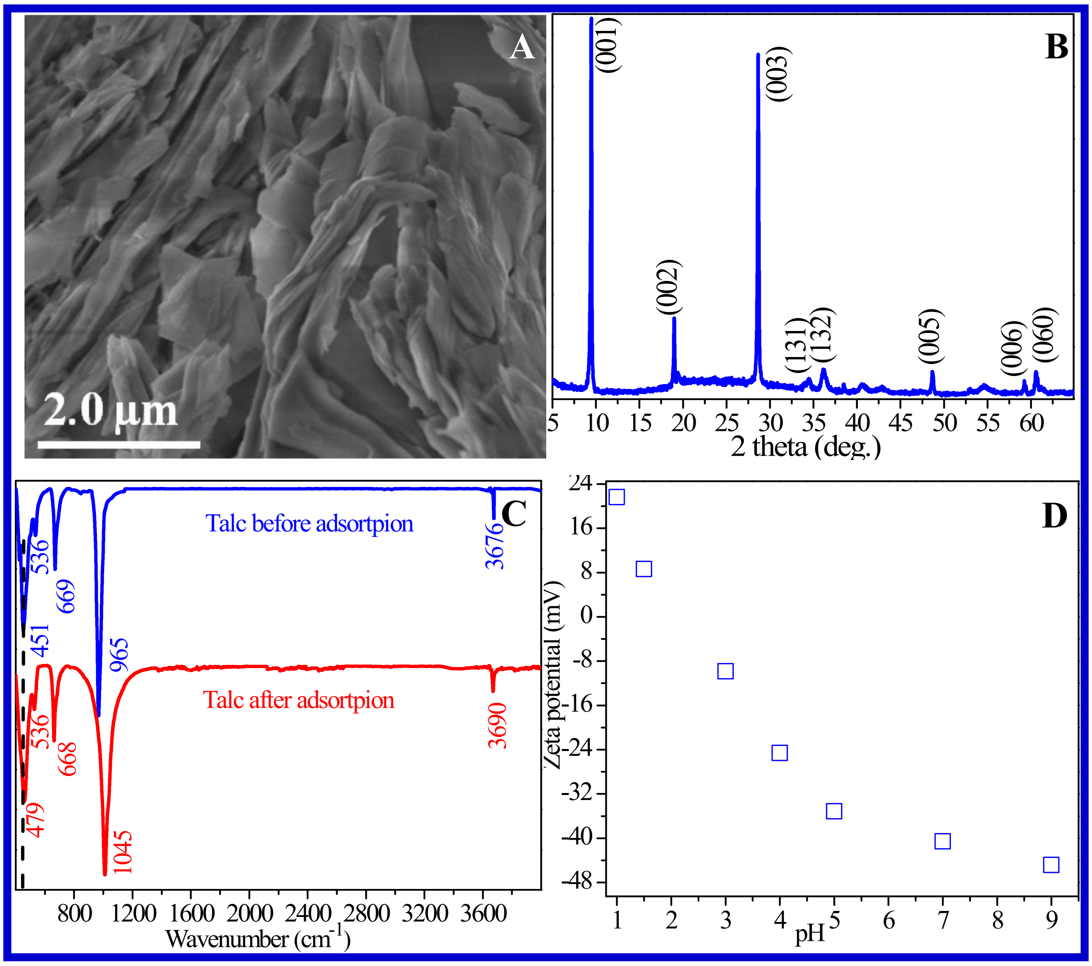

Figure S1. Characterization of Talc. A: SEM image; B: XRD patterns; C: FT-IR spectra; D: zeta-potentials

Distribution Coefficient. Distribution coefficient (K_d, mL/g) was used to determine the affinity of talc for Sr(II)/Cs(I) from aqueous, which can be expressed as Eqn. S1:

$$K_d = \frac{(C_0 - C_e)}{C_e} \times \frac{V}{m} \qquad \text{(S1)}$$

where C_0 and C_e were the Sr(II)/Cs(I) concentrations in the initial solution and in the solution after equilibrium with talc, respectively; V/m is the volume-to-mass ratio.

Adsorption kinetics

The data of adsorption kinetics were fitted by pseudo-first- order and pseudo-second-order kinetic models. The pseudo-first-order and pseudo- second-order kinetic models can be described by Eqns. S2[S2] and S3[S3], respectively:

$$\ln(q_e - q_t) = lnq_e - k_f \times t \qquad \text{(S2)}$$

$$\frac{t}{q_t} = \frac{1}{k_s \times q_e^2} + \frac{t}{q_e} \qquad \text{(S3)}$$

where q_e and q_t (mg/g) are the amount of radionuclides adsorbed at equilibrium and at time t, respectively. k_f and k_s are the pseudo-first order and pseudo-second order kinetic rate constant, respectively. The fitted results and the corresponding kinetic parameters are shown in Figure S2 and Table S3, respectively.

Table S3. The parameters of pseudo-first-order and pseudo-second-order kinetic model of Sr(II) and Cs(I) sorption on talc at single- (Sr(II)_1 and Cs(I)_1) and bi-dilute (Sr(II)_2 and Cs(I)_2) systems

Adsorbates	Pseudo-first-order			Pseudo-second-order		
	qe (mg/g)	kf (min^{-1})	R^2	qe (mg/g)	ks (g/(mg·min))	R^2
Sr(II)_1	3.917	0.0285	0.8187	4.024	0.0452	0.9998
Sr(II)_2	3.729	0.0079	0.8504	1.831	0.0538	0.9998
Cs(I)_1	4.063	0.0109	0.6531	2.306	0.2387	0.9999

Cs(I)_2	3. 477	0.0035	0.6995	0.874	0.3262	0.9998

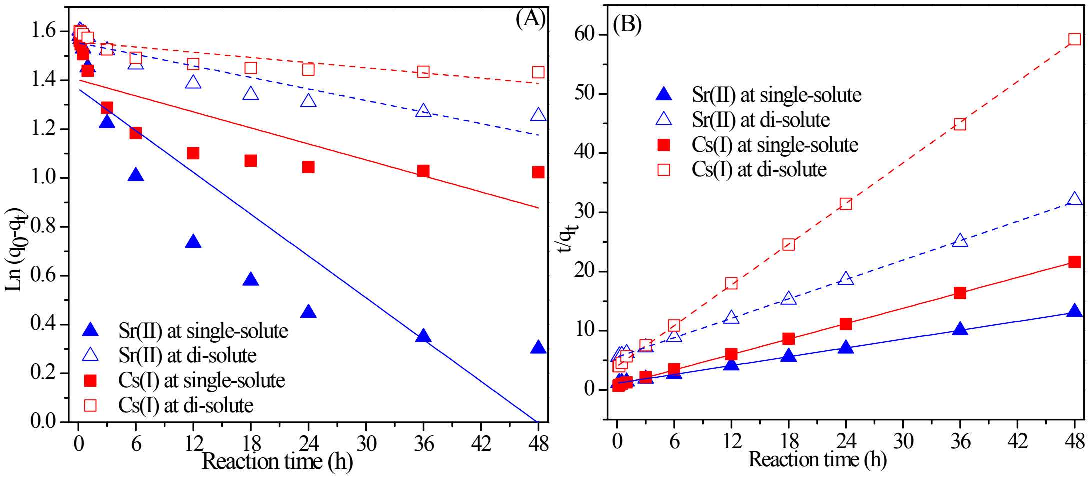

Figure S2. Pseudo-first-order (A) and pseudo-second-order (B) kinetic models of Sr(II) and Cs(I) sorption on talc, pH 5.0, *I* = 0.01 mol/L, m/v = 2.0 g/L, *T* = 293 K.

Langmuir and Freundlich equations

Langmuir and Freundlich model was described by *Eqns.* (S4)[S6] and (S5)[S7], respectively:

Langmuir equation: $$q_e=\frac{q_{max}\times b\times C_e}{1+b\times C_e}$$ (S4)

Freundlich equation: $$q_e=KC_e^{\frac{1}{n}}$$ (S5)

where q_e (mg/g) and C_e (mg/L) are the mass of sorbed radionuclides on talc and Sr(II)/Cs(I) concentration in solution at equilibrium, respectively. b and K are constants of Langmuir and Freundlich model, respectively. $q_{max,}$ (mg/g) are the maximum adsorption capacity at equilibrium.

Table S4. Parameters of Langmuir and Freundlich model for Sr(II) and Cs(I) adsorption onto talc at single- and bi-solute system.

Exp. Conditions	Adsorption isotherms					
	Langmuir			Freundlich		
	K_a (L/mg)	q_{max} (mg/g)	R^2	lnK_F ((mg/g)/(mg/L)^n)	*1/n*	R^2
			Sr(II)			
Single-solute	0.089	11.61	0.9995	1.01	0.3164	0.9673
Bi-solute	0.078	9.99	0.9990	0.6761	0.3574	0.9809
			Cs(I)			
Single-solute	0.047	7.072	0.994	-0.3174	0.4974	0.9815
Bi-solute	0.039	4.214	0.9897	-0.869	0.485	0.9902

Distribution of Sr(II) and Cs(I) in aqueous solutions. The distribution of Sr(II) and Cs(I) in aqueous solutions were calculation by visual MINTEQ mode.[S4]

Table S5. The equilibrium constants of Sr(II) and Cs(I) species in aqueous solutions

Reactions	Log K	Ref.
Sr(II)		
$Sr^{2+} + H_2O = SrOH^+ + H^+$	-5.20	(S4)
$Sr^{2+} + 2H_2O = Sr(OH)_2 + 2H^+$	-11.50	(S4)
Cs(I)		
$Cs^+ + H_2O = CsOH + H^+$	-7.64	(S5)

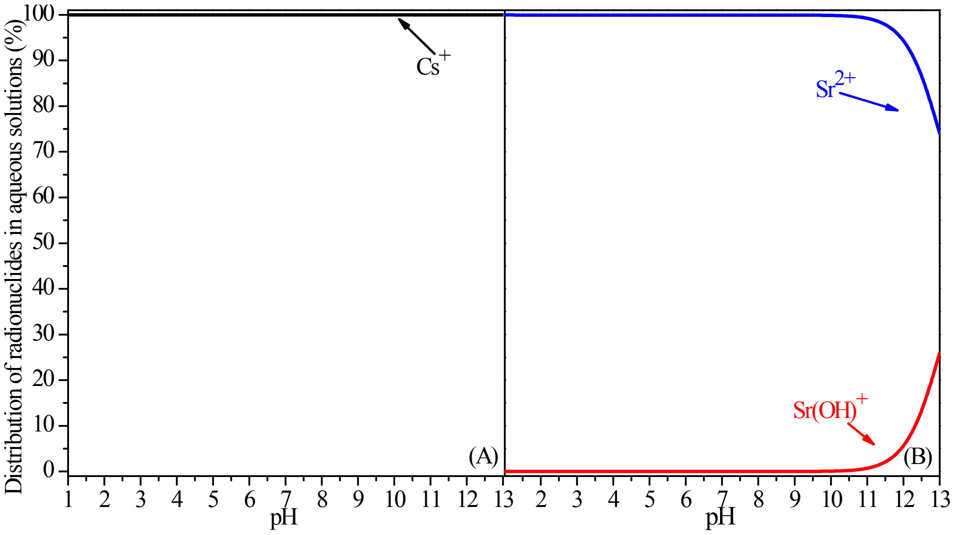

Figure S3. The relative distribution of Cs(I) (A) and Sr(II) (B) as a function of pH in aqueous solutions, $C_0 = 10.0$ mg/L, $I = 0.01$ mol·L^{-1} NaClO$_4$, $T = 293$ K.

XPS Analysis

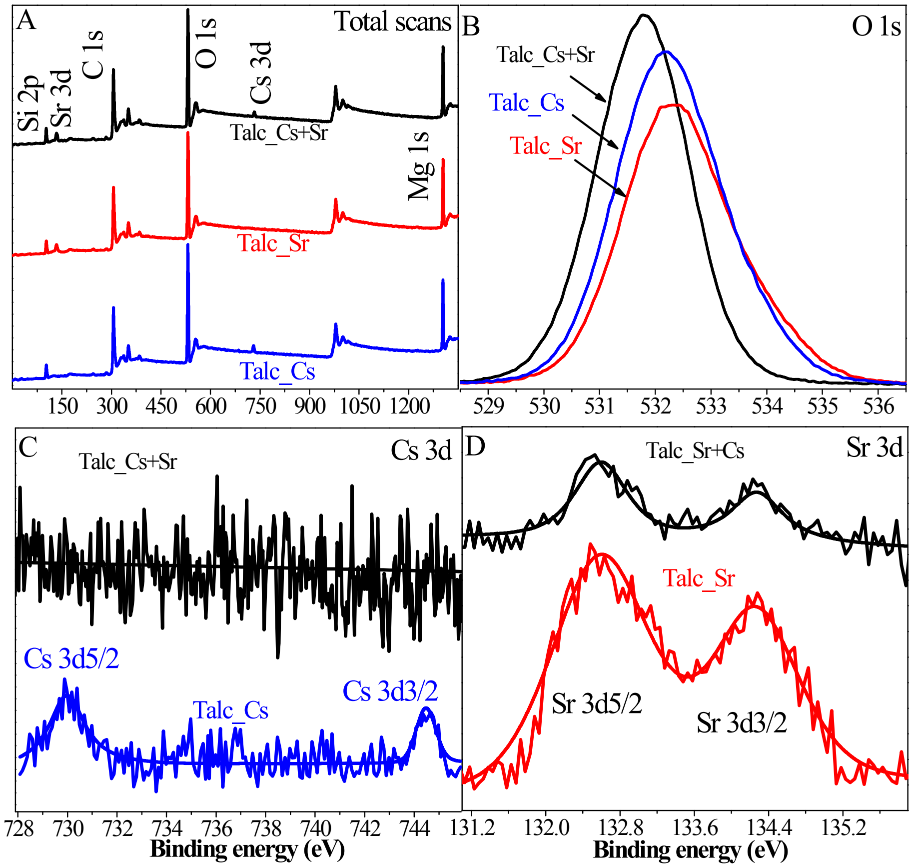

Figure S4. XPS analysis of talc after Sr(II) and Cs(I) adsorption, A: total scans; B: O 1s spectra; C: Cs 3d spectra; D: Sr 3d spectra.

Table S6. Fitted parameters of powder and polarized EXAFS spectra for Sr(II)- and Cs(I)-sorbed Talc

Sample	α	shell	R(Å)[a]	*CN*[b]	σ^{2} [c]
Sr(II)	power	Sr-O	2.60	8.3	0.0025
		Sr-Si	4.10	1.9	0.0034
	10°	Sr-O	2.60[d]	8.26	0.0025[d]
		Sr-Si	4.10[d]	1.95	0.0034[d]
	35°	Sr-O	2.60	8.19	0.0025
		Sr-Si	4.10	1.97	0.0034
	60°	Sr-O	2.60	8.13	0.0025
		Sr-Si	4.10	2.02	0.0034
	85°	Sr-O	2.60	8.15	0.0025
		Sr-Si	4.10	2.11	0.0034
Cs(I)	Power	Cs-O_1	3.15	2.5	0.0013
		Cs-O_2	4.28	4.5	0.0026
	10°	Cs-O_1	3.15[d]	2.3	0.0013[d]
		Cs-O_2	4.28[d]	4.2	0.0026[d]
	35°	Cs-O_1	3.15	2.1	0.0013
		Cs-O_2	4.28	3.9	0.0026
	60°	Cs-O_1	3.15	2.0	0.0013
		Cs-O_2	4.28	3.7	0.0026
	85°	Cs-O_1	3.15	1.9	0.0013
		Cs-O_2	4.28	3.5	0.0026

[a]: interatomic distance; [b]: coordination numbers; [c]: Debye-Waller factor; [d]: Fixed to the value determined at power EXAFS analysis.

Optimized structure of talc

A 2 × 2 supercell of talc [$Mg_3Si_4O_{10}(OH)_2$] model with 84 atoms was built with the unit cell parameters of *a*=*b*=5.347Å, *c*=9.607Å; *α*=*β*=80 °, *γ*=60°.The optimized surface structure can be found in Figure S5.

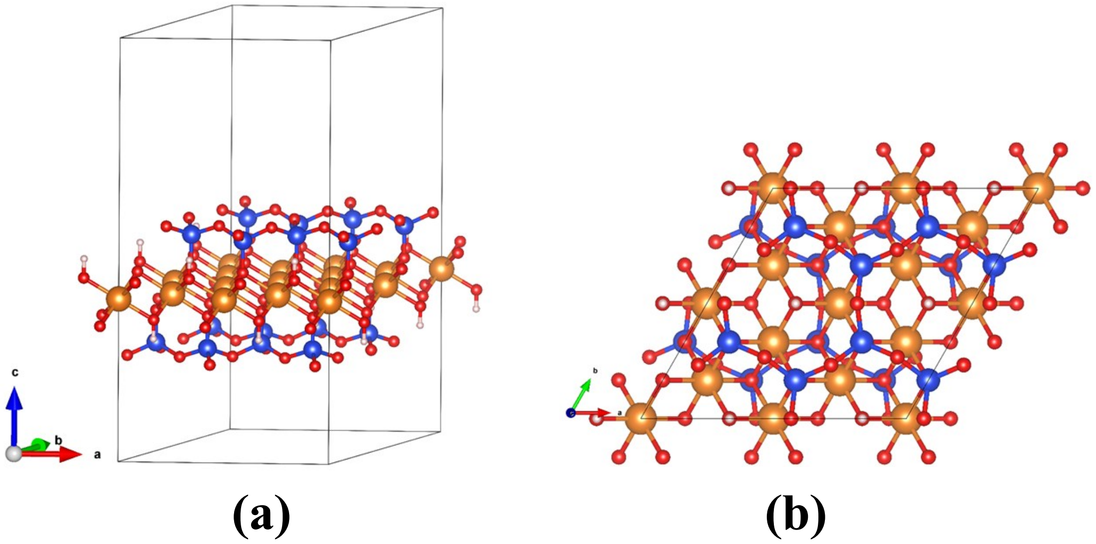

Figure S5. The optimized structure for the [$Mg_3Si_4O_{10}(OH)_2$] surface: (a) side view, (b) top view. Yellow: Mg atom, Blue: Si atom, Red: O atom, and White: H atom.

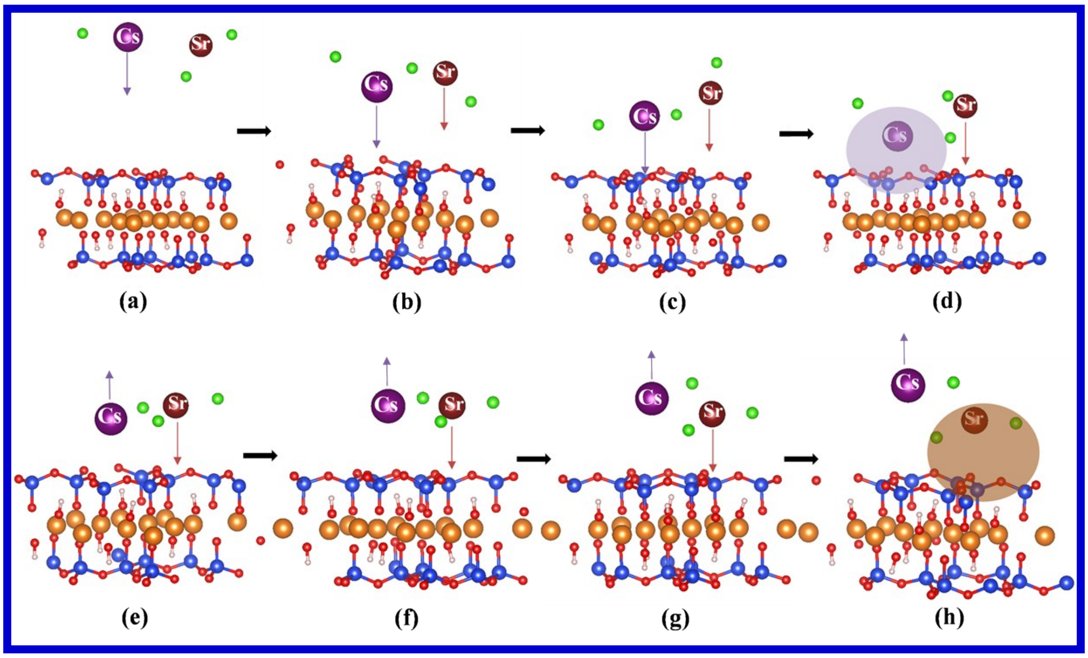

Figure S6. The snapshots of the MD trajectories for the competitive sorption process of Sr(II) and Cs(I). Arrows: the direction of movement.

References

(S1) Lagergren, S. Zur theorie der sogenannten absorption geloster stoffe. Kungliga svenka retenskapsaka demiens, *Handlingar*, **1898**, *24*, 1-39.

(S2) Ho, Y. S. Mckay, G. Sorption of dye from aqueous solution by peat. *Chem. Eng. J.* **1998**, *70*, 115-124.

(S3) van Leeuwen H. P. Dynamic aspects of in situ speciation processes and techniques, In *In situ monitoring of aquatic systems chemical analysis and speciation*; Buffle J., Horvai G., Eds, John Wiley and Sons, Chichester, **2000**.

(S4) Nordstrom, D. K.; Plummer, L. N.; Langmuir, D.; Busenberg, E.; May, H. M.; Jones, B. F.; Parkhurst, D. L. Revised chemical equilibrium data for major water-mineral reactions and their limitation. In *Chemical modeling of aqueous systems II*. (Eds. D. C. Melchior and R. L. Bassett). American Chemical Society Symposium Series,Vol.416, Chap. 31, pp 398-413.

(S5) *NEA. Radionuclide sorption from the safety evaluation perspective. Proceedings of an NEA workshop. October 16-18, 1991. Interlaken, Switzerland.* OECD Publications, Paris, France, **1992**.

(S6) Langmuir, I. The adsorption of gases on plane surface of glass, mica and platinum. *J. Am. Chem. Soc.* **1918**, *40*, 1361-1403.

(S7) Freundlich, H. M. F. Uberdie adsorption in losungen. *J. Phys. Chem.* **1906**, *57*, 385-470.

1. Solbra, S.; Allison, N.; Waite, S.; Mikhalovsky, S. V.; Bortun, A. I.; Bortun, L. N.; Clearfield, A., Cesium and strontium ion exchange on the framework titanium silicate $M_2Ti_2O_3SiO_4{\cdot}nH_2O$ (M = H, Na). *Environ. Sci. Technol.* **2001**, *35*, 626-629.
2. Lagergren, S., Zur theorie der sogenannten adsorption geloster stoffe.Pseudo-second order

model for sorption processes *Handlingar* **1898**, *24*, 1-39.

3. Ho, Y. S.; McKay, G., Pseudo-second order model for sorption processes. *Proc. Biochem.* **1999**, *34*, 451-465.

4. Gustafsson, J. P., A windows version of MINTEQ. *http://http://www.lwr.kth.se/English/OurSOrware/vminteq/index.htm* **2009**.